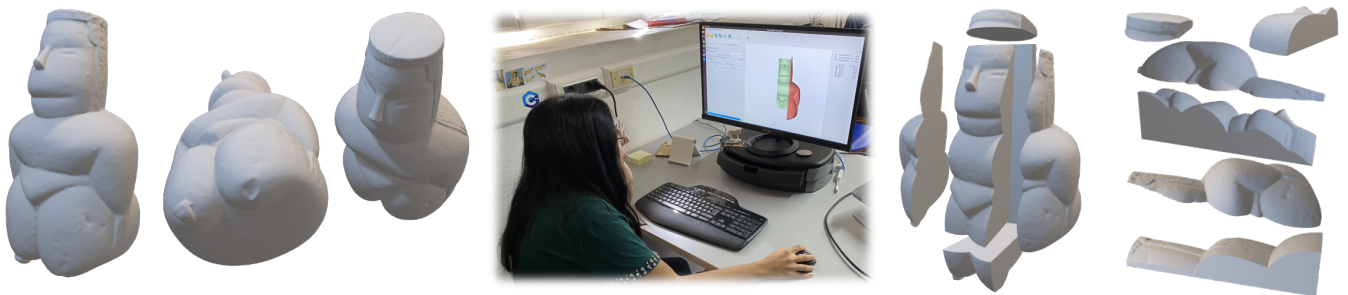# Split and Mill: user assisted height-field block decomposition for fabrication

Alessandro Muntoni [1,2] ⓘ, Lucio Davide Spano[2] ⓘ and Riccardo Scateni[2] ⓘ

[1]Visual Computing Laboratory, ISTI-CNR, Pisa, Italy
[2]Department of Mathematics and Computer Science, University of Cagliari, Italy

Figure 1: *Using Split and Mill the user can interactively look at the digital shape, evaluating which are the best cutting planes to partition it and then generate a subdivision with the guarantee that it is millable with a 3-axis milling machine.*

Abstract

We present here Split and Mill: an interactive system for the manual volume decomposition of free form shapes. Our primary purpose is to generate portions respecting the properties allowing to mill them with a 3-axis milling machine. We show that a manual decomposition is competitive with the automatic partitioning when the user is skilled enough. We, thus, think that our tool can be beneficial for the practitioners in the field, and we release it as free software.

CCS Concepts
• *Computing methodologies* → *Mesh models; Mesh geometry models;* • *Human-centered computing* → *Interaction techniques;*

1. Introduction

Milling machines are a tool in use since more than fifty years in industrial production. They are powerful and reliable, but their versatility is not comparable to the 3D printers, in term of types, models, price range, size and applications. Thus, using milling machines to fabricate in a single pass free-form objects of any shape respecting the constraints given by the very nature of the machine is still a challenge. The main constraint is given by the need to lay the milled part on a flat bed. This implies to have the portion of material under fabrication to be flat on the side opposite to the milling tool. An algorithm for free-form fabrication should, then, decompose the shape in portions that are flat on one side and can be milled on the opposite. An automatic algorithm that computes such decompositions has been proposed [MLS*18], but their results lack

practical manufacturability for complex models. We designed and implemented *Split and Mill*: a novel interactive system that can let the user decompose any shape giving her or him hints on the correct partition in relation to the milling process. We believe that our tool will be practically useful. *Split and Mill* gives the user the ability to produce a valid decomposition, which is also practical for manufacturing. With the help of the user, it allows obtaining decompositions of models where the automatic state of the art approaches do fail or compute valid but unfeasible decompositions. We conducted a user test to evaluate the usability of our tool. We are positive that our results are an interesting testbed for understanding where future research on automatic decomposition should aim to be competitive with manual interaction.

2. State of the art

Volume decomposition of three-dimensional shapes is a sector of research of interests in different fields.

Woo and Sakurai [WS02] propose a divide-and-conquer approach, based on the volume of the parts, to perform feature recognition of mechanical parts. Zhang and colleagues [ZJR18] applies methods of machine learning, in particular, convolutional neural networks to solve the same problem of feature recognition. As for the other proposal, it analyzes only objects characterized by the regularity of their shapes: faces planar or with constant curvature and sharp angles, often right.

Gao and colleagues [GMD*16] present, instead, a proposal for the decomposition of free-formed shapes. They use a sweeping approach that partitions the volume in cuboids, following the idea of polycube decomposition introduced in [THCM04] that are computable with approaches like the one in [LVS*13]. The approach works for any shape, but it has few or no control for the shape and size of the portions. Fanni and colleagues [FCM*18] explore the manufacturability for additive and subtractive techniques of decompositions induced by polycubes. Their decompositions are not suitable for 3-axis milling machines.

Since we are interested in obtaining parts respecting special constraints, we compare ourselves with state-of-the-art methods for automatic volume decomposition of free forms in parts that are millable with 3-axis milling machines as [MLS*18]. The main goal of Muntoni and colleagues is to obtain an overlap-free decomposition of a 3D shape in blocks that meets several constraints for manufacturing purposes. The algorithm can be set for the computation of decompositions manufacturable with 3-axis CNC milling machines or 3D printing without external supports.

We try to solve the same problem, but with a slightly different pipeline manually executed by the user. In our approach, the user creates a set of boxes that sequentially cut manufacturable blocks, and the manufacturing constraints are checked in real-time. Therefore, since the boxes are generated and cut sequentially, we don't need to resolve overlaps, and we can use non-axis-aligned boxes. Despite our approach being user assisted and not automatic, an expert user is able to obtain better decompositions than [MLS*18] both in number of blocks and quality of the decomposition controlling where are the cuts in the input surface.

There are several commercial and free software for digital fabrication; most of them are focused on 3D printing (e.g., [Ult], [Sim], [Mat]). These software allow editing 3d models for additive manufacturing purposes interactively. Most of the interactive software for subtractive fabrication are concentrated on the manipulation of regular objects like mechanical parts or, more generally, models represented with CAD formats. Some software also support free-form geometries (e.g., [Aut]), but they allow only to generate and simulate manufacturing tool-paths. They don't allow to edit or decompose meshes.

3. GUI Description

Figure 2 presents the main window of *Split and Mill*, which is designed to give the user all the tools to build a suitable decomposition
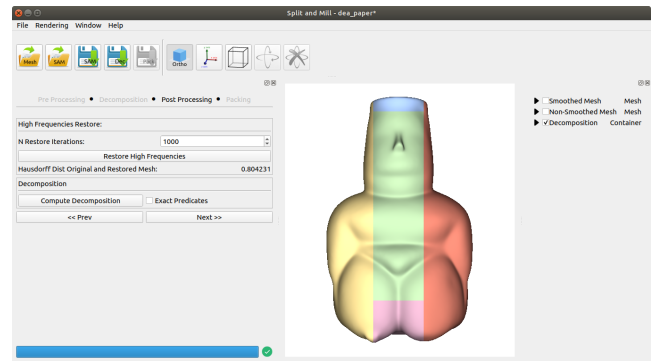

Figure 2: *Graphic user interface of Split and Mill.*

of a 3D shape suited for fabrication purposes. We divided the main window in four parts, listed into the next paragraphs.

Since our application provides several tools that may require some time for their computations, a progress bar is placed in the bottom-left of the window. It will give feedback to the user whenever a heavy operation is being executed.

Top Bar. The top bar lists a set of push buttons. They allow performing some operations that are available in more than one step of the pipeline. They are divided into two categories: the first one allows to load or save both 3D meshes or decomposition projects in a file format suited for our purpose. The second category contains buttons to control some rendering settings of the 3D viewer (e.g., orthographic v.s. stereoscopic camera, the possibility to draw the main axis or an axis aligned box), and to enable the manual rotation mode. The latter allows the user to manually perform a rotation of the input mesh at the beginning or also during the decomposition. All the functions of these buttons are also available in the drop-down menu.

Pipeline dialog. The pipeline dialog contains all the instruments that allow the user to build the desired decomposition, allowing him to understand which task of the pipeline is performing at any point in time. The dialog shows one of four possible tabs, depending on the task that the user is performing. Its title highlights the current task name. Each tab contains buttons, spin boxes, and other GUI controls useful to perform all the possible operations that can help the user to reach his goal. Whenever possible, all controls are set with default values. The next section will deeply describe all the tabs.

3D Viewer. The 3D viewer allows renders all the objects present in the 3D scene and it supports the user in interacting with them. It uses the virtual trackball rotation system to manipulate the objects. It exploits an orthographic view by default, that suits better our application purposes. Indeed, orthographic view shows, from every point of view and at every zoom level, only the portion of surface that can be reached from a milling tool.

View options dialog. The View options dialog contains a list of checkboxes and subframes that allow the user to control the visibility and the rendering options of every object contained in the scene.

4. Pipeline overview

Our application allows obtaining valid volumetric decompositions of 3D shapes suitable for fabrication using 3-axis milling machines or 3D printers with no supports.

The primary geometric constraint that a block needs to satisfy for 3-axis CNC milling machine is that it has to be a height-field with a flat base w.r.t. a defined milling direction. Additive manufacturing relaxes this strict constraint, allowing the fabrication of more complex surfaces. However, it is possible to obtain better 3D printed results, avoiding external supports that may dirty critical portions of the model surface [LEM*17]. Our tool is suited for securing decomposition for both additive and subtractive manufacturing. For additive manufacturing, our tool allows obtaining volumetric decompositions where every block can be manufactured without supports, knowing the overhang angle of the 3D printer used for the fabrication. For CNC 3-axis milling, our application allows obtaining volumetric decompositions composed of blocks that meet manufacturing constraints.

To be valid, a decomposition should meet the following requirements:

- blocks do not overlap each other;
- all the blocks jointly cover the entire surface of the mesh;
- every block has an assigned milling (printing) direction;
- every block has a flat base orthogonal to its milling direction;
- the surface of every block (except its base) does not exceed a given flip angle.

The flip angle will be 90 degrees for subtractive technologies (the block will have a height-field surface) or the overhang angle of a 3D printer for additive technologies.

The only requirement on the input is that it should be a closed surface. Our application guides the user to follow a well-defined pipeline. The main idea to obtain valid decompositions is to consecutively cut volume blocks of the input shape that satisfy the manufacturing constraints. The user can cut these blocks computing consecutive boolean subtractions between the input surface and a manipulable 3D box, checking in real-time if the contained volume satisfies the manufacturing constraints. The consecutive intersections and subtractions of all the boxes generated will then result in a valid decomposition.

In practice, our application guides the user through a pipeline, showing at each step a tab containing all the tools useful for every task. Each of the four consecutive pipeline stages is associated with a tab that is shown in the pipeline dialog. The steps are the following:

- Pre-processing
- Decomposition
- Post-processing
- Packing

Every tab contains a set of tools which can be used by the user to perform every operation that he wants to achieve. All the actions can be undone and redone using the popular universal shortcuts when it deemed necessary. We describe all the four tabs and the operations they allow to perform in the next subsections.

Figure 3: *The pre-processing tab. From top to bottom: two spin boxes to set the angle tolerance parameters; a frame for the optional high frequencies removal trough a Taubin Smoothing with given parameters; a frame for finding a sub-optimal initial orientation of the shape (starting from a pool of a given number of directions), a frame to test show the flip colors w.r.t. a given milling direction.*

4.1. Pre-processing

Once the user loads a 3D mesh, the pre-processing tab is shown in the pipeline dialog (Figure 3). The user can now select some parameters and perform some optional operations.

The user is asked to select two tolerance values, which will be used during the manual decomposition: a *light tolerance angle* value, and a *flip angle* value. Light tolerance is used mostly for visual feedback, and a flip angle value is used for preventing unwanted cuts during the manual decomposition. Changing the flip angle values allows the user to use either relaxed or hard constraints for height-field decomposition, or also to set the overhang angle for decompositions suited for 3D-printing without supports. Default values are proposed for height-field block decompositions with a tolerance of 5 degrees.

There are two proposed and optional operations that might be useful for obtaining good decompositions. The first proposed operation is to reduce the high frequencies of the input 3D shape, as done in [MLS*18], allowing the user to sacrifice exact fidelity of the fabricated shape, that may make severe the manual decomposition process. The applied filter is the one proposed in [Tau95], and high frequencies will be restored in the post-processing tab.

Another proposed pre-processing step consists of computing a sub-optimal orientation of the input shape, using the same RANSAC approach used in [MLS*18]. The user then is always allowed to modify the orientation of the input shape by pushing the manual rotation button situated in the tab bar of the main window.
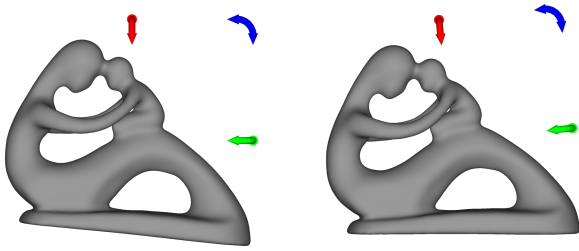
Figure 4: *Usage of the manual rotation tool on a non-oriented fertility model (left). Dragging the blue arrow, the user can perform a rotation along the z axis and orient the model as he prefers (right).*

Figure 5: *Difference of flipping surface w.r.t. x axis on the dea model before (left) and after (right) high frequencies removal. With this visualization, the user can immediately understand, for example, if high frequencies removal is necessary.*

The manual rotation button is available in the pre-processing and decomposition steps of the pipeline. During manual rotation, all the other functions are disabled until the user completes the rotation. When the user presses the manual rotation button, three draggable colored arrows appear around the mesh. The arrows allow the user to perform a rotation along one of the three principal axes, depending on the arrow dragged. When the user thinks that the manual rotation is completed, he can push another time the manual rotation button. An example of manual rotation usage can be found in Figure 4.

The user can immediately see the results of tolerance values and high frequencies removal by enabling the colored visualization of the mesh w.r.t. one of the major axis, checking the "Color Orientation Triangles" checkbox. Figure 5 shows an example of the described visualization. Triangles having an angle between their normal and the chosen axis higher than flip angle, higher than tolerance angle and below tolerance angle are colored respectively with red, yellow and green. With this visualization, the user can understand if the pre-processing operations computed are enough to ensure a proper decomposition (e.g., if the number of smoothing iterations is sufficient, or if the model has been properly rotated), and therefore if she or he is ready to start the manual decomposition.

When the user is satisfied with the performed pre-processing operations, and it is ready to start the decomposition, he can push the "Next" button.

4.2. Decomposition

The decomposition task of the proposed pipeline asks the user to cut a set of blocks from the input shape. In practice, this task helps the user to produce an ordered set of axis-aligned 3D boxes. These boxes, if sequentially intersected with the input shape (that may change orientation between the boolean operations), will produce a valid decomposition that meets the constraints given in the pre-processing tab.

When the user finishes all the pre-processing operations, the decomposition tab will be shown (Figure 6), and a manipulable 3D axis-aligned box appears in the viewer (Figure 7). The sizes of the box can be modified by dragging with the mouse two spheres at its extremes. Through the apposite radio buttons placed in the decomposition tab, the user can select the milling direction associated with the box (which is shown near it).
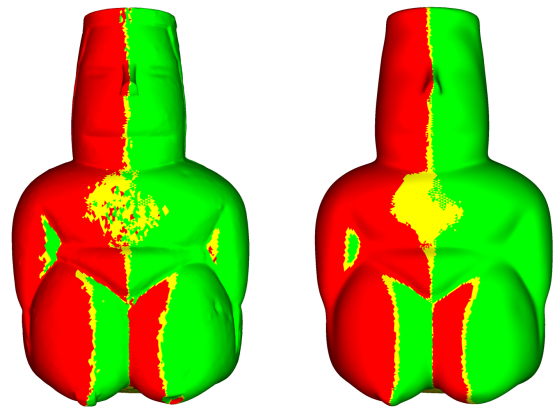
This box allows the user to cut blocks that will become part of the decomposition. When the box has the right sizes and only covers a portion of the surface that can be manufactured, the user can push the "cut" button. The application will perform an exact difference operation [ZGZJ16] between the actual mesh and the box, and the result will become the new mesh. The application stores the box involved in the boolean operation in a list that, in the post-processing tab, will allow obtaining the actual decomposition. The user can iterate the cut operations until it is satisfied, though a correct decomposition should cover the entire surface of the input shape. To achieve this goal, the user can see at any time of the task the percentage of remaining surface and the residual volume of the actual mesh in the decomposition tab. Figure 8 shows an example of the possible steps of a decomposition task performed in the *dea* model.

During the task, the user can color all the triangles of the mesh or the triangles contained in the box, according to the selected milling direction. This possibility helps the user understand if the box covers triangles that can or cannot be manufactured (w.r.t. the tolerances and constraints selected in the pre-processing tab).

Modifying sizes of the box by dragging its extremes with the cursor makes it impossible to control the exact coordinates of every block. This aspect may be problematic in a situation where two or more boxes should have faces that lie each other or should be aligned along a coordinate. In this case, the user can use the guides checkboxes of the decomposition tab. They show dashed lines along all the directions checked for every coordinate of the previous detached boxes, and the user can snap the current box at the nearest desired coordinate. A usage example of the guides can be found in Figure 9.

At every time of the decomposition task, the user can manually rotate the current mesh by pushing the rotation button in the top bar and performing a manual rotation. A list of rotations is saved
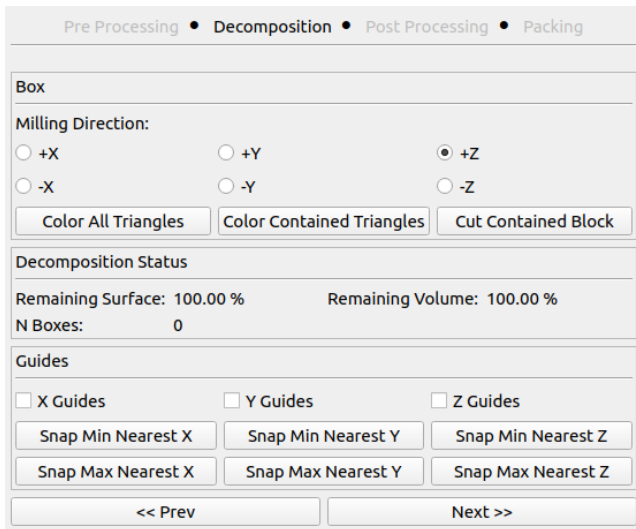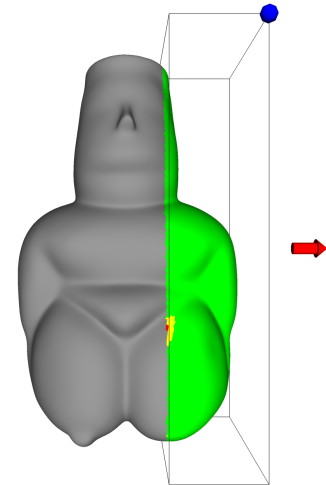
Figure 6: *The decomposition tab. From top to bottom: a set of radio buttons for selecting the milling direction associated to the box; three push buttons that allows respectively to color all the mesh according to the selected direction, color only the triangles contained in the box and cut the block contained in the box; some information regarding the actual state of the decomposition; a frame containing controls to show guides and snapping the box to specific coordinates; buttons that allow to move in the previous or next step of the pipeline.*

Figure 7: *The dea model partially covered by the manipulable box during the manual decomposition. The user can change the sizes and the position of the box dragging the spheres positioned in the corners of the box (one sphere is occluded by the mesh). The arrow shows the milling direction selected by the user, and the triangles covered by the box are colored according to the chosen angle tolerances.*

alongside the list of boxes computed by the user and used when the actual blocks of the decomposition will be computed. The possibility of rotating the mesh allows us to obtain non-axis-aligned decompositions that cannot be obtained using [MLS*18] approach. This aspect is discussed in Section 5.

4.3. Post-processing

When the user finishes the decomposition task, the post-processing tab is visualized (Figure 10), allowing the user to obtain the actual decomposition after an optional operation of restoring high frequencies. The frame for the high frequencies restore is enabled if they were removed before the decomposition task. As in [MLS*18], the high frequencies restore tool reintroduces the high frequencies where it is possible, according to the constraints given by the direction associated with every block, and the *flip angle* chosen. The user can control the number of iterations of the minimization, and he can visualize the Hausdorff distance [CRS98] between the original and the restored surface mesh.

After restoring high frequencies, the user is ready to compute the actual decomposition of the input surface. Given the ordered list of boxes, they are sequentially detached from the restored shape, also repeating rotations if there have been during the decomposition task. The user can choose to use CGAL's exact predicates [The19] if deemed necessary. This option is not defaulted due to the long times required.

4.4. Packing

Once all the post-processing tasks are completed, and the actual decomposition is computed, a set of utility tools for the packing of the decomposition are provided, making then the object ready to be manufactured. All the utilities are available in the packing tab (Figure 11), which will appear when the user finishes the post-processing tasks.

The user is asked to insert the sizes of stock. The stock is a 3D box that will contain the blocks of the decomposition rotated correctly in such a way that the block base is aligned to the *xy* plane. The 3D box can be considered as the sizes of the starting stock if the decomposition is suited for subtractive manufacturing, or the 3D printing chamber if it is suited for additive manufacturing. For subtractive manufacturing, it may be useful for practical reasons to leave a frame in the stock (e.g., used to secure the stock to the machining tray) or to leave a height offset in the base of the stock (to avoid the milling tool touching the machining tray). In this scenario, the user can also compute, for every packing, its negative. That may be manufactured and then used to remove the base offset from the manufactured decomposition precisely.

After rotating the blocks to align their bases to the *xy* plane, the blocks are resized to make every block manufacturable with the given milling tool length (if it applies) and making the biggest block fit in the sizes of the stock. Since an optimal packing of decomposition is not the purpose of this paper, we used a simple 2D bin packing algorithm applied on rectangles (the 2D bounding boxes of the rotated blocks). Applying the 2D bin packing to the decomposition, the 3D viewer will show a set of packings containing all the blocks of the decomposition. If the user is not satisfied with the number of packings obtained, she or he can apply a scale factor (default value is 1). The scale factor will resize all the blocks and
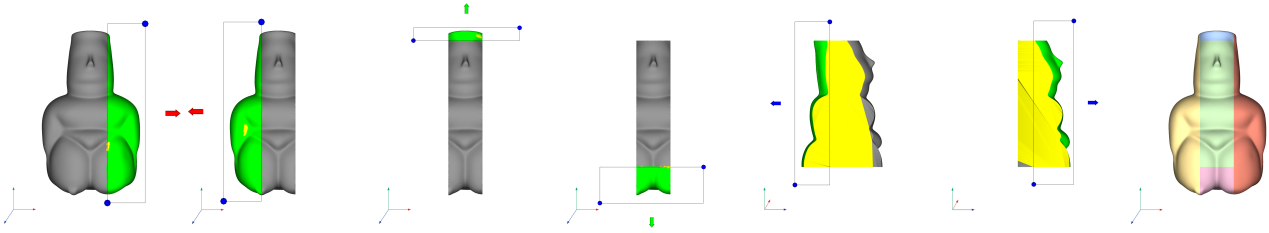
Figure 8: *Decomposition of the dea model using 6 blocks. At every step, the user moves, resizes and change the milling direction of the box, detaching consecutive blocks.*
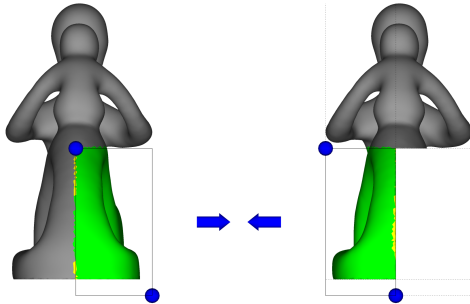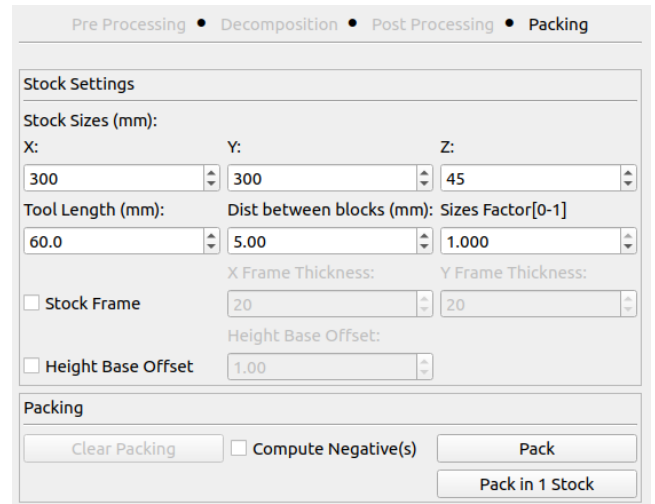

Figure 9: *Usage of guides in the Fertility model. After detaching the first box (left), the coordinates of the second box can be aligned to the first, by showing the dashed lines and then snapping the box to the desired coordinates (right).*
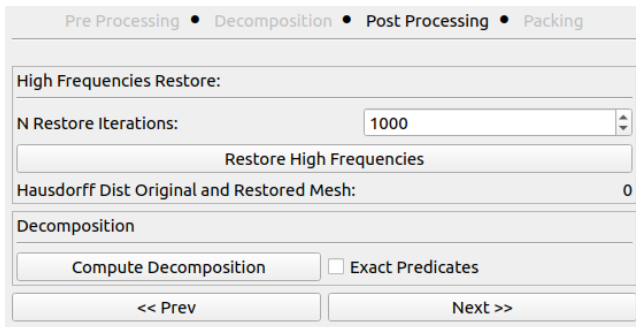
Figure 10: *The post-processing tab. From top to bottom: a frame for the high frequencies restore, with a spin box to control the number of restore iterations, and a value indicating the Hausdorff distance between the input mesh and the restored mesh; a frame for computing the actual decomposition.*

Figure 11: *The packing tab. From top to bottom: a frame from the settings of the stock that will contain the packing and other settings for placing the blocks inside it (minimum distance between blocks, stock frame, height base offset, etc.); a packing frame that allows to pack the blocks in a set of packings or a single packing resizing the blocks accordingly.*
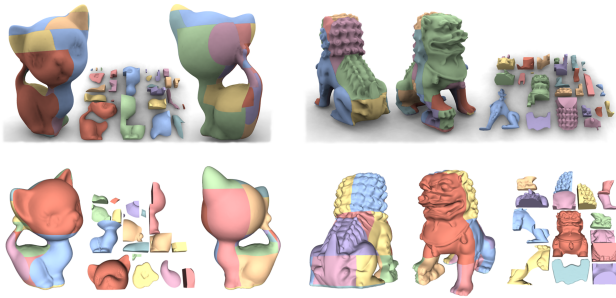
5. Results

In this section, we present a series of resulting decompositions suited for 3-axis CNC milling obtained with *Split and Mill*. Our goal was to get valid height-field block decompositions minimizing the number of blocks and avoiding, when possible, to have cut along critical parts of the input model.

We compare our results with [MLS*18], showing that *Split and Mill* makes possible to obtain decompositions with significant improvements in the number of blocks in most of the shapes (Table 1), especially on complex models like *kitten*, *chinese lion* (Figure 12) and *fertility* (Figure 13). For complex models, the decomposition task required a long time to be completed, showing that the task can be arduous also for expert users. The main difference between [MLS*18] and our method is that they first find an unordered set of boxes, and then they try to find a sorting of these boxes, splitting them if necessary. This pipeline would be extremely hard to be computed by a user. In our approach, the user does not need

consequently decreases the number of packings. If the user wishes to obtain a single packing containing all the blocks, she or he can push the button "Pack in 1 stock". The application will find the maximal scale factor that produces a single packing.

When the user is satisfied by the computed packing, he can export it in the main 3D surface formats, ready to be manufactured.

Model	# Blocks [MLS*18]	# Blocks Ours	Time
Airplane	11	4	7 min
Batman	8	8	12 min
Bimba	16	9	19 min
BU	9	9	18 min
Buddha	8	10	25 min
Chinese lion	27	15	23 min
Dea	7	5	8 min
Fertility	63	23	45 min
Kitten	25	18	32 min
Laurana	10	7	11 min
Lincoln	14	8	9 min
Max Plank	8	7	10 min
Moai	12	2	4 min

Table 1: *Model statistics: A list of model decomposed with [MLS*18] method and ours, comparing the number of blocks. We list also the time required to manually decompose every model.*

Figure 13: *Decomposition of the fertility model obtained with our method. After decomposing most of the model and leaving only a portion of the arm, the user changed the rotation of the model in order to cut it using less blocks.*

to resolve overlaps between boxes, because she or he cut portions of volume sequentially. Therefore, there is no need to find a valid sorting of the boxes since it is intrinsic in the sequence of boxes.

Figure 12: *Comparison between kitten (left) and chinese lion (right) models, decomposed with [MLS*18] (up) and our method (down).*
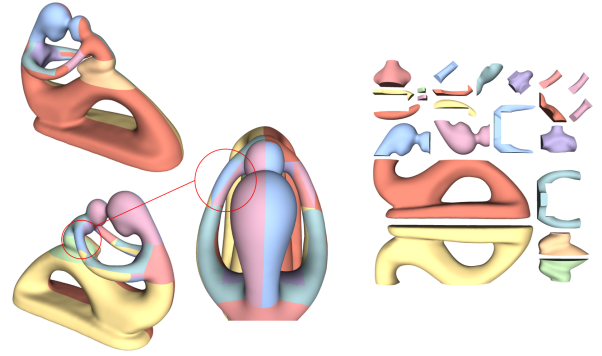
Our approach makes simpler the management of non-axis-aligned cuts, that can be made by manually rotating the shape during the decomposition. This feature has been crucial during the decomposition of the fertility model since the user was able to align to the major axis the two arms of the model and split them in a low number of blocks, as shown in Figure 13. However, in the showed results most of the time was enough to use the manual rotation only before beginning the decomposition.

A gallery of the resulting decompositions obtained with *Split and Mill* is shown on Figure 14.

6. User Test

We conducted a preliminary evaluation for assessing the usability and the effectiveness of the decomposition interface. The objective is to ensure that users who have a basic experience with 3D model editing and manipulation can complete a decomposition for fabricating a mesh having a medium complexity.

We organised the study in three sections. In the first one, the users

were introduced to the tool through a tutorial video showing the decomposition of the moai model. The video explained the tool features completing a concrete decomposition example. After this introduction phase, the users started the first autonomous decomposition on a simple model (the *dea* model). Then, they carried out another decomposition task on a more complex model, the *Max Planck*. We selected the two models considering the expected number of cuts for decomposing them, trying to avoid trivial models and complex ones that would require too much time for the participants. The *dea* model is the simplest, requiring about 5 cuts, while the *Max Planck* requires at least two more cuts. We consider a task completed when the user covered the whole surface in the decomposition. At the end of each task, the participants filled a NASA TLX [Har88]. Finally, the participants completed the session filling a post-test questionnaire, consisting of a set of questions on the different tool features. We collected the time spent on each task and we saved the decompositions created by the users.

Fourteen people participated in the evaluation 13 male and 1 female. Their age ranged between 23 and 34 years ($\bar{x} = 27.8$, $s = 3.4$). They had a high instruction level: 3 hold a bachelor degree, 8 a master and 3 a PhD. They had a good knowledge on 3D mesh editing ($\bar{x} = 4.3$, $s = 2.0$ in a 1 to 7 Likert scale) with a sufficient knowledge on fabrication techniques ($\bar{x} = 3.4$, $s = 2.2$).

All participants successfully completed all tasks, covering the whole surface of the two proposed models. Figure 15 shows all the decompositions created by the participants in the second task. They used about 7 cuts in both tasks ($\bar{x}_1 = 6.6$, $s_1 = 2.3$, $\bar{x}_2 = 6.8$, $s_1 = 1.5$). While in the first one the number of cuts was higher than needed, in the second they reached the expected number, showing that the experience with the first model helped them in finding a good strategy for the second.

The users spent on average more time in decomposing the simpler model ($\bar{x}_1 = 16$min 22s, $s_1 = 8$min 26s) than in decomposing the more complex one ($\bar{x}_2 = 9$min 5s, $s_2 = 5$min 0s) and the difference was significant ($t(13) = 4.11$, $p = .001$, $c.i. = [3$min 27s; 11min 6s$]$). We found a practically significant difference in the task load, measured through the NASA-TLX, but its absolute value is about 6%, so
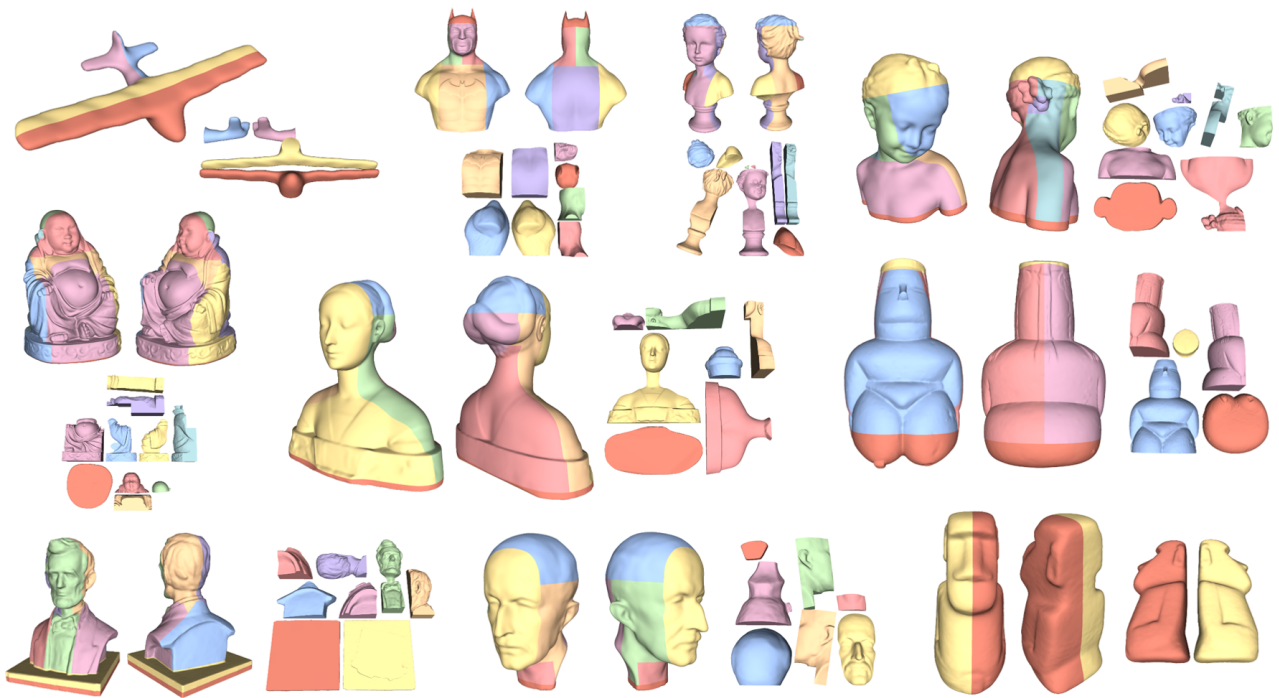
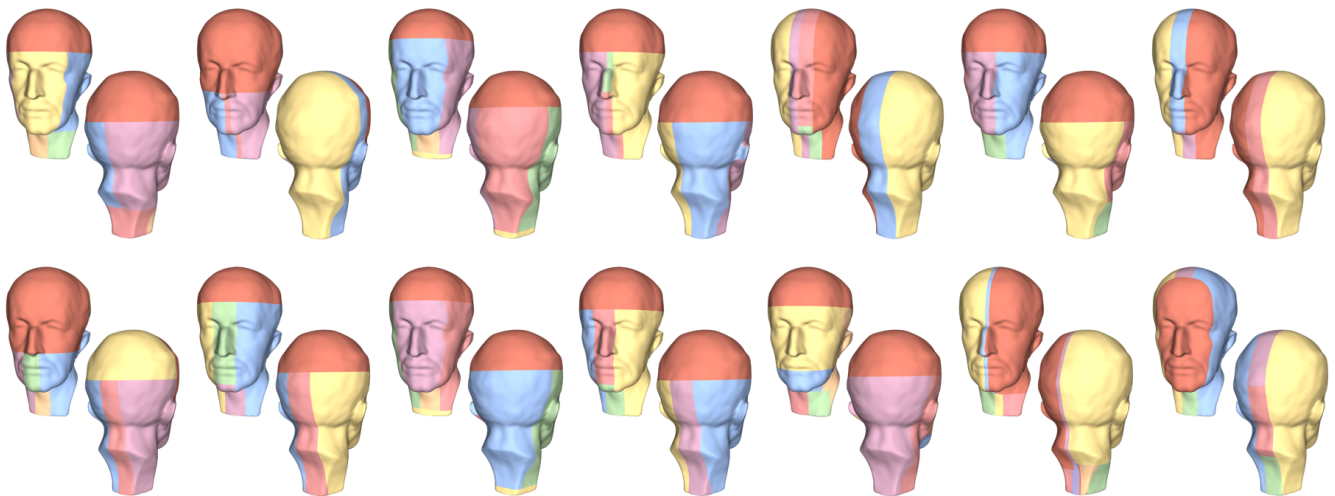**Figure 14:** *A gallery of some models decomposed using our method.*

**Figure 15:** *All the 14 different decompositions of the Max Planck model computed during the user tests.*

the difference is hardly perceivable for the user if compared with the one registered on the task time($\bar{x}_1 = 29.52$, $s_1 = 14.50$, $\bar{x}_2 = 22.68$, $s_2 = 15.68$, $t(13) = 1.88$, $p = .08$, $c.i. = [-1.00, 14.7]$). The explanations for the higher time spent versus a comparable load are basically two. First, as expected, the participants used the first task for learning how the tool works and spent time in exploring the features and figuring out how to perform the operations. Second,

lacking a way for undoing an operation, half participants requested to restart the decomposition after completing some exploratory cuts, which explains the higher time spent on task. So, the lack of an undo command configures as the main usability problem of the tool. It affected the completion time without increasing too much the load.

Such conclusion reflects in the NASA-TLX dimensions. We reg-

istered a significant difference only in the effort required to the user ($t(13) = 2.37$, $p = .03$, $c.i. = [1.3, 26.6]$), which was higher when he required to restart the decomposition. However, considering the absolute value of the NASA-TLX results, the load of the decomposition task is reasonable, as highlighted also in the post-test comments and the participants were able to tune their strategy already in the second task. Figure 16 summarizes the value of each dimension included in the load index.
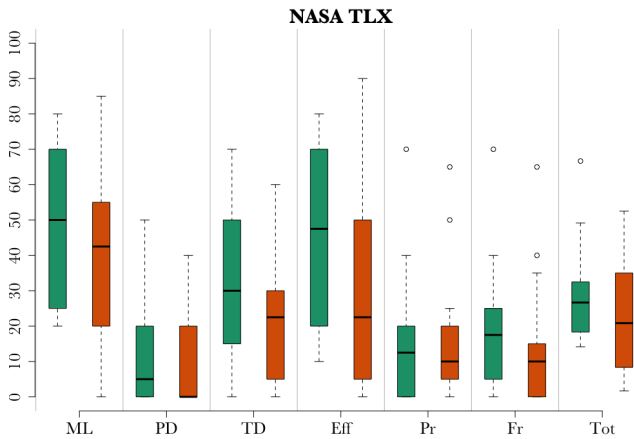

Figure 16: *Results of the NASA-TLX [Har88] ratings for T1 (decomposing the dea model) and T2 (decomposing the Max Planck model). We report the overall difficulty evaluation (Tot) and the six factors considered in the questionnaire: mental demand (MD), physical demand (PD), temporal demand (TD), effort (Eff), the overall performance (Pr) and frustration level (Fr). The Pr dimension has been reversed for consistency with the other dimensions (the lower, the better).*

In the post-task questionnaire we asked the participants to rate the following features in a 1 to 7 Likert scale:

- Visualization of the millable portion of a model along a given direction (Dir);
- Surface simplification through smoothing (Smt);
- Setting the decomposition box (Box);
- Simulating a cut (Cut);
- Using the snapping guides for setting a cut (Gd);
- Restoring details after the decomposition (Res)
- Decomposition visualization (Vis)
- Overall evaluation on the application (App);

Figure 17 shows the results of the post-test questionnaire. The ratings show a good acceptance of the proposed interface. The support for setting the decomposition box received consistently a lower score if compared with the other features. The participants required more guidance for understanding which parts of the box allowed its positioning. Some of them suggested placing a handle on each vertex of the box. Also, they would like an update on the millable portion visualization each time they move the box. The participants highlighted also some problems in using the snapping guides. They would like support for selecting and visualizing them directly in the canvas, without using the radio buttons in the right-hand panel.

On the positive side, the participants considered the overall application interface simple to use and learn, explicitly stating that after the first usage they were proficient in the decomposition task. They were able to reuse the experience they had with other 3D modelling tools for exploring the model, even if they expected more real-time updates during the manipulation of the decomposition box.
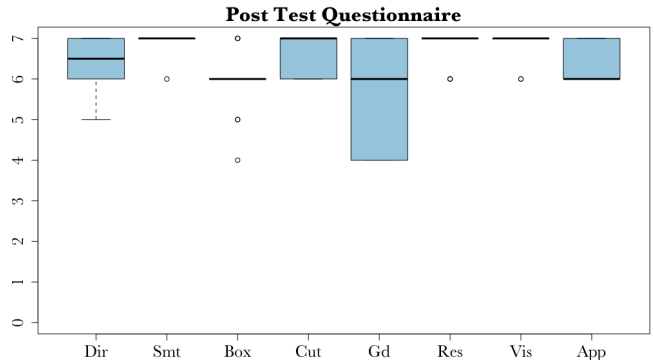
Figure 17: *Post-test evaluation of the application features (1 to 7 Likert scale, the higher the better).*

In conclusion, the participants considered the tool effective and simple to use for people having experience in 3D modelling. The evaluation highlighted three important improvements that the tool requires. First, it needs the support for undoing and redoing operations, to be completely compliant with the direct manipulation paradigm. Second, the decomposition box needs more support for interactive actions. This includes adding more handles and modes for easier and quicker positioning and a real-time update of the milling portion visualization while moving. Third, the snapping guide feature needs improvements in its effectiveness.

7. Conclusions and future works

We presented *Split and Mill*: a novel user-guided algorithm for the decomposition of closed surfaces in blocks suited both for additive or subtractive manufacturing. Our goal was to propose an interactive application that could be used for computing decompositions when the automatic approach proposed by [MLS*18] fails on producing feasible or good-looking solutions. With our tool, we computed several decompositions that are better in terms of quality and number of blocks, giving practical value to the application. Although we cannot show the optimality of our results due to the complexity of the addressed problem, we can state that they can be used to compare future fully automatic approaches.

User Test. We performed a user test of the application to evaluate the usability of the system and to establish if it is a simple or challenging problem for the user to produce a decomposition. All users completed all the tasks and they increased their performance through the considered tasks. The participants showed a good acceptance of the proposed interface, requesting more features supporting trial-and-error strategies.

Future Works. As for future works, we firstly plan to manufacture a few models to prove the feasibility of our decompositions for both additive and subtractive manufacturing. We also plan to integrate a set of features to our application to improve the user experience. As suggested by the users who participated in the test, we plan several feature additions to our tool. The most requested ones where, for example, to automatically update the coloring of the triangles contained by the box during the decomposition process, separating the surface triangles from triangles generated by a cut using different colors and an automatic snapping of the box if guides are enabled.

Implementation Details. We implemented *Split and Mill* in C++, using *Eigen* ([GJ*10]) for linear algebra routines, *cg3lib* ([MN*18]) for the core application, *libigl* for mesh booleans ([ZGZJ16], [JP*18]), *vcglib* for some pre-processing routines [C*16]. The entire project works and is tested in all the three main desktop operative systems (Microsoft Windows, macOS, and Linux Ubuntu), and compiles with GCC, Clang, and MSVC. The source code of the application is available for the download at the following link: github.com/cg3hci/SplitAndMill.

References

[Aut]	AUTODESK: Autodesk fusion 360. URL: https://www.autodesk.com/products/fusion-360/. 2

[C*16]	CIGNONI P., ET AL.: vcglib: A C++, templated, no dependency, library for manipulation, processing and cleaning of triangle meshes, 2016. URL: https://github.com/cnr-isti-vclab/vcglib. 10

[CRS98]	CIGNONI P., ROCCHINI C., SCOPIGNO R.: Metro: measuring error on simplified surfaces. In *Computer Graphics Forum* (1998), vol. 17, Wiley Online Library, pp. 167–174. 5

[FCM*18]	FANNI F. A., CHERCHI G., MUNTONI A., TOLA A., SCATENI R.: Fabrication oriented shape decomposition using polycube mapping. *Computers & Graphics 77* (2018), 183–193. 2

[GJ*10]	GUENNEBAUD G., JACOB B., ET AL.: Eigen v3, 2010. URL: http://eigen.tuxfamily.org. 10

[GMD*16]	GAO X., MARTIN T., DENG S., COHEN E., DENG Z., CHEN G.: Structured volume decomposition via generalized sweeping. *IEEE Transactions on Visualization and Computer Graphics 22*, 7 (July 2016), 1899–1911. doi:10.1109/TVCG.2015.2473835. 2

[Har88]	HART, SANDRA G. AND STAVELAND, LOWELL E.: Development of NASA-TLX (Task Load Index): Results of Empirical and Theoretical Research. In *Human Mental Workload*, vol. 52 of *Advances in Psychology*. 1988, pp. 139 – 183. 7, 9

[JP*18]	JACOBSON A., PANOZZO D., ET AL.: libigl: A simple C++ geometry processing library, 2018. URL: https://libigl.github.io/. 10

[LEM*17]	LIVESU M., ELLERO S., MARTÍNEZ J., LEFEBVRE S., ATTENE M.: From 3d models to 3d prints: an overview of the processing pipeline. In *Computer Graphics Forum* (2017), vol. 36, Wiley Online Library, pp. 537–564. 3

[LVS*13]	LIVESU M., VINING N., SHEFFER A., GREGSON J., SCATENI R.: Polycut: Monotone graph-cuts for polycube base-complex construction. *ACM Trans. Graph. 32*, 6 (Nov. 2013), 171:1–171:12. doi:10.1145/2508363.2508388. 2

[Mat]	MATERIALISE: Materialise magics. URL: https://www.materialise.com/en/software/magics. 2

[MLS*18]	MUNTONI A., LIVESU M., SCATENI R., SHEFFER A., PANOZZO D.: Axis-Aligned Height-Field Block Decomposition of 3D Shapes. *ACM Trans. Graph. 37*, 5 (Oct. 2018), 169:1–169:15. 1, 2, 3, 5, 6, 7, 9

[MN*18]	MUNTONI A., NUVOLI S., ET AL.: CG3Lib: A C++ geometry processing library., 2018. URL: https://github.com/cg3hci/cg3lib. 10

[Sim]	SIMPLIFY3D: Simplify3d. URL: https://www.simplify3d.com/. 2

[Tau95]	TAUBIN G.: Curve and surface smoothing without shrinkage. In *Computer Vision, 1995. Proceedings., Fifth International Conference on* (1995), IEEE, pp. 852–857. 3

[THCM04]	TARINI M., HORMANN K., CIGNONI P., MONTANI C.: Polycube-maps. *ACM Trans. Graph. 23*, 3 (Aug. 2004), 853–860. doi:10.1145/1015706.1015810. 2

[The19]	THE CGAL PROJECT: *CGAL User and Reference Manual*, 4.14 ed. CGAL Editorial Board, 2019. URL: https://doc.cgal.org/4.14/Manual/packages.html. 5

[Ult]	ULTIMAKER: Ultimaker cura. URL: https://ultimaker.com/it/software/ultimaker-cura. 2

[WS02]	WOO Y., SAKURAI H.: Recognition of maximal features by volume decomposition. *Computer-Aided Design 34*, 3 (2002), 195 – 207. doi:https://doi.org/10.1016/S0010-4485(01)00080-X. 2

[ZGZJ16]	ZHOU Q., GRINSPUN E., ZORIN D., JACOBSON A.: Mesh arrangements for solid geometry. *ACM Transactions on Graphics (TOG) 35*, 4 (2016), 39. 4, 10

[ZJR18]	ZHANG Z., JAISWAL P., RAI R.: Featurenet: Machining feature recognition based on 3d convolution neural network. *Computer-Aided Design 101* (2018), 12 – 22. doi:https://doi.org/10.1016/j.cad.2018.03.006. 2